Wuhan University
Journal of Natural Sciences

2022, Vol.27 No.2, 177-184

Article ID 1007-1202(2022)02-0177-08
DOI https://doi.org/10.1051/wujns/2022272177

Antitumor Response of Anti-B7-H3 CAR-T Cells with Humanized scFv in Solid Tumors

☐ SI Ke[1], XU Huantian[1],YE Zheng[1], JAFFAR ALI Doulathunnisa[1], HE Cong[1], DING Bo[2], YUAN Shubin[3], DAI Zhu[1], LI Zhanping[1], SUN Bo[1], SHEN Yang[2†], XIAO Zhongdang[1†]

1. School of Biological Science and Medical Engineering, Southeast University, Nanjing 210096, Jiangsu, China;

2. Zhangda Hospital, School of Medicine, Southeast University, Nanjing 210009, Jiangsu, China;

3. Jiangsu Yinfeng Biological Technology Co. Ltd, Nanjing 210014, Jiangsu, China

Abstract: We prepared a humanized alternative B7-H3 CAR (B7-H3-haCAR-T) targeting B7-H3 which contained the humanized singl-chain varinlde fragment (scFv) from humanized 8H9 Monoclonal Antibody (hu8H9mAb). The antitumor effects of B7-H3-haCAR-T cells were evaluated in B7-H3 overexpressed tumor cells (*in vitro*) and B7-H3 xenograft models (*in vivo*). The specific tumour killing ability of B7-H3-haCAR-T in overexpressing B7-H3 tumour cells was verified by cytotoxicity and ELISA tests. In addition, B7-H3 haCAR-T cells were also noted to suppress the tumour growth remarkably well in the xenograft murine models, and the survival time in the haCAR-T cell treatment group was appreciably longer than that in the control group. The specific recognition and highly efficient tumoricidal behavior of B7-H3 haCAR-T provide a basis for future clinical studies with humanized scFv-transduced CAR-T cells targeting solid tumors.

Key words: humanization; single-chain variable fragment (scFv); B7-H3; haCAR-T; solid tumor

CLC number: Q 819

Received date: 2022-01-07

Foundation item: Supported by the National Natural Science Foundation of China (81671807), the Key Research & Developement Program of Jiangsu Province (BE2020777), Fundamental Research Funds for the Central Universities (2242018K3DN05, 2242021k10004)

Biography: SI Ke, male, Ph.D. candidate, research direction: tumor immunotherapy, chimeric antigen receptor T-cell immunotherapy. E-mail: 15345437340@163.com

† To whom correspondence should be addressed. E-mail: zdxiao@seu.edu.cn; shenyang0924@sina.cn

0 Introduction

Chimeric antigen receptor (CAR) T cells are T lymphocytes genetically modified to express a synthetic receptor that induces T cell activation and costimulatory pathways when combined with cell surface antigens on tumor cells[1]. The CAR allows T cells to be directed to a range of tumor cells surface antigens with high specificity, independent of major histocompatibility complex (MHC) restriction and antigen processing, thereby bypassing the main mechanisms of tumors escape from immune recognition[2]. Selection of the single-chain variable fragment (scFv) of extracellular antigen-binding domain in the structural design of CAR is critical which directly determines the efficiency and assurance of CAR-T therapeutics[3]. Majority of currently applied scFvs are derived from previously published sequences of heavy and light chain of mouse monoclonal antibodies (mAbs)[4]. Yet, many researchers have demonstrated that the host immune responses identify mouse scFv phenotypes and annul the consequent CAR-T infusions[5-7]. In order to overcome this, humanization strategies have been designed to replace the segment of mAbs with human counterparts. Satisfyingly, the humanized alternative CD19 CAR is superior to its murine counterpart in terms of antigen-binding affinity and *in vitro* antitumor efficacy[8]. Thus humanized alternative CAR-T cells have the feasibility to smash the impediment induced by immunogenicity of murine scFv after multiple infusion of murine CAR-T cells.

B7-H3, a type I transmembrane protein, located on human chromosome 15, belongs to B7 family which has two isoforms of the extracellular domain called 4IgB7-H3 and 2IgB7-H[9]. Recent evidence suggests that B7-H3 is broadly overexpressed in most human malignancies and limitedly expressed in normal human tissues[10, 11].

On the other hand, the increased enrichment of B7-H3 in tumor cells is often associated with less tumor infiltrating lymphocytes, quicker development of cancer, and worse clinical outcome of various malignant tumors[12-14]. Added, various B7-H3-specific mAbs agents have shown promising antitumor activity and safety in clinical trials[15, 16]. Taking altogether, B7-H3 has been considered and recommended as a good target for CAR T-cell immunotherapy.

8H9mAb is a murine IgG1 which has been reported to target B7-H3[17]. By immunohistochemistry, 8H9mAb has been shown to extremely reactive with a variety of human solid tumors and to display positive tumor absorption capacity in the xenograft models of brain and sarcoma tumors[18, 19]. In multiple clinical trials, 8H9mAb has been tested as a safe and effective target for the radioimmunotherapy of leptomeningeal metastases (NCT00089245)[20], diffuse intrinsic pontine glioma (NCT01502917)[21] and peritoneal metastases (NCT01099644)[22]. Interestingly, B7-H3 CAR-T derived from the 8H9mAb has shown potent anti-tumour effects in the treatment of glioblastoma[23]. In addition, a newly developed humanized 8H9mAb (hu8H9mAb) has been tested to have potent antitumor activity and thus it might modulate the immunomodulatory properties of B7-H3[24].

Herein, we developed a new B7-H3-targeting CAR by means of a B7-H3 scFv from humanized 8H9mAb and assessed its safety and effectiveness against B7-H3 overexpressed tumor cells (*in vitro*) and B7-H3 xegraft murine models (*in vivo*). Our results indicated that the humanized scFv from hu8H9mAb may be an attractive scFv for CAR-T treatment of solid tumors in the future.

1 Materials and Methods

1.1 Cell Lines and Culture Media

SGC and 293T cell were obtained from ATCC. The B7-H3-SGC-Mcherry cell line was produced by transfection of the parental SGC cells with lentivirus vector pLVX-B7-H3-Mcherry-N1, which had been previously constructed in our laboratory. The transfected SGC cells were then labelled with anti-human B7-H3 antibody (BioLegend) and classified to obtain a community of B7-H3 over-expressing SGC cells.

SGC, B7-H3-SGC-mCherry and 293T cells were cultured in Dulbecco's modified Eagle medium(DMEM) supplemented with 10% fetal bovine serum (FBS), 100 U/mL penicillin, and 100 mg/mL streptomycin. Human peripheral blood mononuclear cells (PBMCs) were cultured in RPMI-1640 medium with 10% FBS, IL-2 (50 ng/mL), 100 U/mL penicillin, and 100 mg/mL streptomycin. All cells were kept in 5% CO_2 at 37 ℃. All of the above cell culture media and ingredients were acquired from Hyclone.

1.2 Construction of CAR Vector and Retrovirus Production

The CAR sequence including signal peptide, humanized scFv targets B7-H3, hinge, CD8 TM, the cytoplasmic structural domains of human CD28, 4-1BB and CD3ζ was synthetically prepared by Genescript (China) and was cloned into a lentivirus vector (pLVX-EF1α-IRES-ZsGreen-N1).

Lentiviral vectors were generated by instantaneous transfection of 293T cells utilizing standard calcium phosphate precipitation protocol. In brief, 293T cells cultured in 10 cm culture dishes were transfected with 12 μg of the lentiviral backbone plasmid, along with 9 μg of the psPAX2 and 3 μg of the pMD2.G packaging plasmids. The viral supernatants were harvested 48 h and 72 h of post-transfection and filtered through a 0.45 μm filter, then ultracentrifuged at 20 000 r/min for 2 h at 4 ℃. The obtained granules were resuspended in chilled phosphate buffered saline (PBS) and kept at −80 ℃ until used.

1.3 T Cell Transduction and Expansion

Human peripheral blood mononuclear cells (PBMCs) were separated from the blood of a healthy donor by density gradient centrifugation, cultured in RPMI-1640 with 10% FBS and IL-2 (50 ng/mL). PBMCs were stimulated by incubating the cells with human T-activator CD3/CD28 beads for 24 h prior to retroviral transduction (bead:cell ratio was 1:1). For transduction, lentivirus supernatant was spin-loaded onto 12-well plates coated with 18 mg/mL RetroNectin (Takara) and centrifuged 2 h at 2 000 g at 32 ℃. The supernatant was discarded and activated T cells (5×10^5 cells/well) were added to the plates loaded with vector along with fresh medium. The plates were centrifuged at 2 000 r/min 32 ℃ for 5 min and cultured overnight at 37 ℃ and 5% CO_2. During *in vitro* amplification, the medium was supplemented and the cell density was adjusted to 5×10^5 -1×10^6/mL for every 2 days.

1.4 Flow Cytometry and Western Blot Analysis

The successful surface expression of B7-H3-haCAR on T cells was detected with the help of flow cytometry. In brief, the cells were washed with 1% FBS contained PBS, incubated with the antibody for 20 min at 4 ℃ in the dark followed by twice PBS (containing 1% FBS) washing and then continued with analysis using BD C6

flow cytometry and with FlowJo software. B7-H3-haCAR-T cells co-expressing ZsGreen protein were detected in FITC Texas green channel, and B7-H3-haCAR expression on the surface of T cells was evaluated by applying anti-mouse $F(ab)_2$-APC antibody (Abcam).

Western blot was performed to verify B7-H3-haCAR protein expression. T cells (2×10^6) were incubated in 100 μL lysis buffer (RIPA) and afterward centrifuged at 12 000 g for 20 min at 4 ℃. Protein concentrations were analysed through a BCA protein assay kit (TaKaRa). Around 40 μg of protein were loaded onto 10% SDS-PAGE which were transferred to PVDF membrane (Millipore) after separation and then incubated with anti-human CD3ζ (Santa Cruz) primary antibody overnight. Afterward the blot was incubated with horseradish peroxidase (HRP)-conjugated secondary antibody (Santa Cruz) for 2 h and the bands were detected by ECL Western Blotting Analysis System (Tanon 4600).

1.5 Cytotoxicity Assays

Cytotoxicity assay was examined by employing ^{51}Cr assay as described[23]. In brief, 0.1 mCi (3.7 MBq) ^{51}Cr was added to the target cells (10^6/mL) and placed at 37 ℃ water bath for 1 h. The labelled target cells and effector cells were then mixed according to an E:T ratio of, 10:1, 5:1, and 1:1. After 4 h, the supernatants were collected and radioactivity was examined by a WIZARD2 gamma counter (Perkin-Elmer). The percentage of specific lysis was calculated by the following formula: (test release−spontaneous release)/(maximal release−spontaneous release)×100.

Cytokine release assay was achieved by a co-incubation of 8×10^4 T cells with 1.6×10^4 target cells (E:T ratio, 5:1) per well in 96-well-plate (three parallel samples per well. After 12 h, supernatants were examined for IFN-γ and IL-2 production with ELISA kit (MULTI SCIENCES).

1.6 *In vivo* Study on Anti-Tumor Efficacy of AR-T Cells in Xenograft Mouse Model

Xenograft tumor mouse model was established by subcutaneous flank injections of 6×10^6 B7-H3-SGC-Mcherry cells in 6-week-old female BALB/c nude mice (Shanghai Lab Animal Research Center). When the tumor reached about 300 mm^3 in 7 days after tumor cells inoculation, the mice were divided into three groups (5 per group) and injected with 1×10^7 T cells of different groups/150 μL (B7-H3-haCAR-T cells, T cells, and PBS) via tail vein. Tumor growth was monitored once in two days and tumor volume was calculated using the formula: $1/2\times\text{length}\times(\text{width})^2$. The time of death of each group of mouse was recorded to plot survival curves using GraphPad Prism software v.8.0.

1.7 Statistical Analysis

All the data were expressed as the mean±standard deviation. Histograms and line charts were generated by GraphPad Prism 8.0. T tests were used to determine the *P* values. The *P* values were used ($^*P<0.05$, $^{**}P<0.01$, $^{***}P<0.001$).

2 Results

2.1 Construction and Detection of B7-H3-haCAR-T Cells

To generate B7-H3-specific T cells, B7-H3 targeted third-generation CAR was first prepared and the CAR encoding fusion protein has the following protein sequences: IgG κ leader peptide, humanized B7-H3 scFv, the hinge, TM region of human CD8α, intracellular signal domain of 4-1BB, CD28 costimulatory domain, the CD3ζ chain, an Internal ribosome entry site (IRES) and ZsGreen (Fig.1(a)). The successful haCAR expression on T cells following lentivirus transduction was examined by the co-expression of ZsGreen (which is under the control of IRES) using fluorescence microscope (Fig. 1(b)) and flow cytometry (Fig.1(c)). The haCAR protein expression on T cells was also simultaneously checked with western blot. In addition to the endogenous CD3ζ (15 ku) band which was detected in both NT (non-transduced) and CAR-T cells, a protein band of approximately 60 ku was also observed in CAR-T cells (Fusion haCAR protein matches expected dimensions), but not in NT cells which confirmed the successful construction of haCAR-T cells (Fig.1(d)). Further, following 14 days of lentiviral transduction, the phenotypic categories of haCAR-T cells were examined using flow cytometry (Fig.1(e) and (f)). Surprisingly, a ratio of 1:7 of CD4+/CD8+ T cells were counted in the flow cytometry analysis which clearly confirmed that the large proportion of T cells were CD8+ T cells. In addition, T cell markers such as the central memory phenotypic markers (CD45RO, CCR7) and exhaustion phenotypic markers (PD-1, TIM3) were also inspected to confirm the phenotypic categories of the haCAR-T cells. But there was no noteworthy disparity found in the expression of the above mentioned T cell markers between the haCAR-T and NT cell groups.

2.2 Anti-tumor Effect of B7-H3-haCAR-T Cells *in vitro*

To find the anti-tumor effect of B7-H3-haCAR-T cells both *in vitro* and *in vivo*, B7-H3 overexpressed B7-

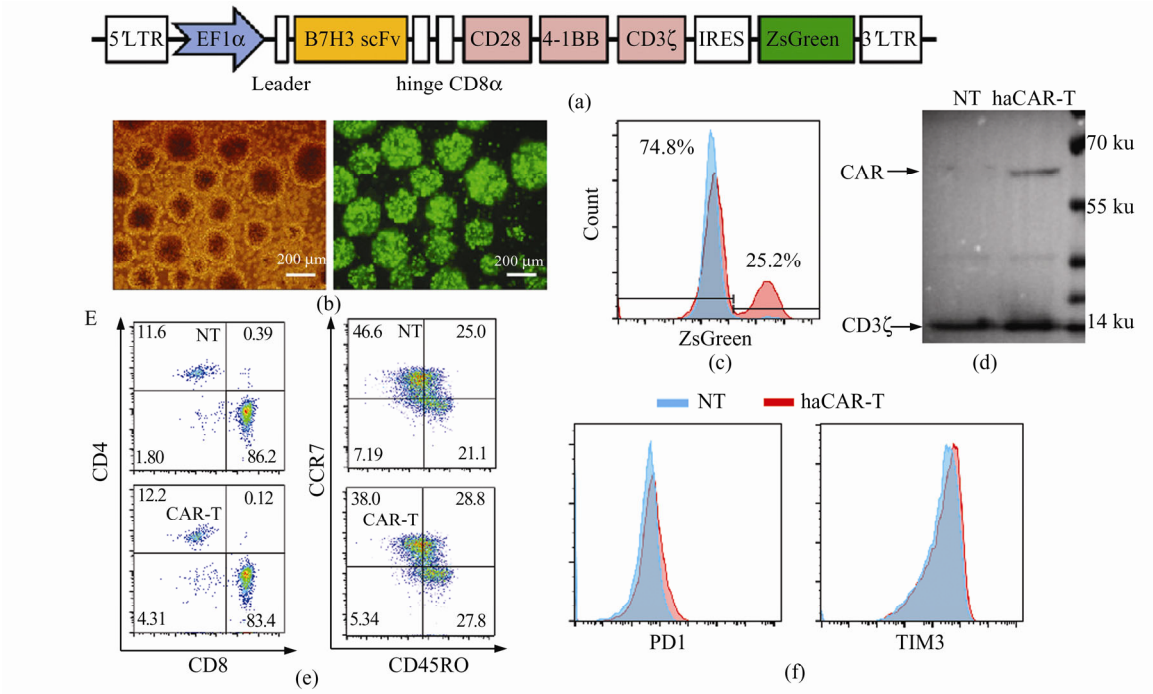

Fig. 1 Manufacture of B7-H3-haCAR-T cells

(a) Scheme of B7-H3-haCAR which comprises of anti-B7-H3 scFv, the hinge and transmenbrane (TM) region of human CD8α, CD28 and 4-1BB signaling domain, human CD3ζ chain, IRES and ZsGreen. (b) and (c) The expression effectiveness of haCAR was detected through (b) fluorescent microscope and (c) flow cytometric assay of ZsGreen. Flow cytometry detected 25.2% of total T cells expressing ZsGreen. (d) Immunoblot analysis of cell lysates from both untransduced and CAR transduced T lymphocytes. (e) and (f) Phenotypic categories of NT and haCAR-T cells were determined by flow cytometric analysis after 14 days of lentiviral transduction

H3-SGC-Mcherry (B7-H3-SGC-M) cells were prepared via molecular biology methods. Later, flow cytometry analysis was utilized to confirm the cell surface expression of B7-H3 in B7-H3-SGC-M cells (Fig. 2(a)), during which the B7-H3-negative cells SGC-Mcherry(SGC-M) were used as a control. To assess the specific anti-tumor effect of B7-H3-haCAR-T cells, firstly, the cytotoxic effect of B7-H3-haCAR-T cells was tested using ^{51}Cr release cytotoxicity assay. As shown in Fig. 2(b), haCAR-T cells proficiently and specifically lysed B7-H3-overexpressed B7-H3-SGC-M cells; in contrast, there was no major response noted in B7-H3 negative SGC-M cells. Next to find out the relative cytokine secretion level, B7-H3-SGC-M and SGC-M cells were co-incubated with haCAR or NT cells at an effector to target cells (E:T) proportion of 5:1, from which the supernatants were collected and tested with ELISA kit. As expected, an increase in the release of interleukin-2 (IL-2) and interferon-gamma (IFN-γ) was detected in the supernatant of B7-H3-SGC-M cells co-incubated with haCAR-T cells, which was not the case in SGC-M cells (Fig. 2(c)). This confirmed that the haCAR-T cells have potent anti-tumor efficacy. Furthermore, subsequent analysis was performed to examine the tumour-killing capacity of B7-H3-haCAR-T cells at low E:T proportion *in vitro*, during which haCAR-T cells were co-incubated with B7-H3-SGC-M or SGC-M cells at an E:T proportion of 1:6. After 72 h of co-incubation, the remaining haCAR-T and tumour cells were counted using flow cytometry. The results revealed that more B7-H3-SGC-M cells were lysed by B7-H3-haCAR-T cells compared to SGC-M cells (Fig. 2(d) and (e)). This result evidenced that co-culturing of B7-H3-haCAR-T with B7-H3-SGC-M cells significantly increased the expansion rate of B7-H3-haCAR-T than the SGC-M cells (Fig. 2(e)).

2.3 Antitumor Effect of B7-H3-haCAR-T Cells *in vivo*

Having proved the specificity and functionality of B7-H3-haCAR-T cells *in vitro*, *in vivo* antitumor effect was evaluated subsequently. A subcutaneous B7-H3-SGC-Mcherry cells xenograft model was established to investigate the anti-tumor effect of B7-H3-haCAR-T cells *in vivo* by injecting B7-H3-SGC-7901 cells (1×10^6) into the flank of female nude mice (n=5 per treatment group). When the average tumor volume reached about 100 mm^3, the mice were then injected with 1×10^7

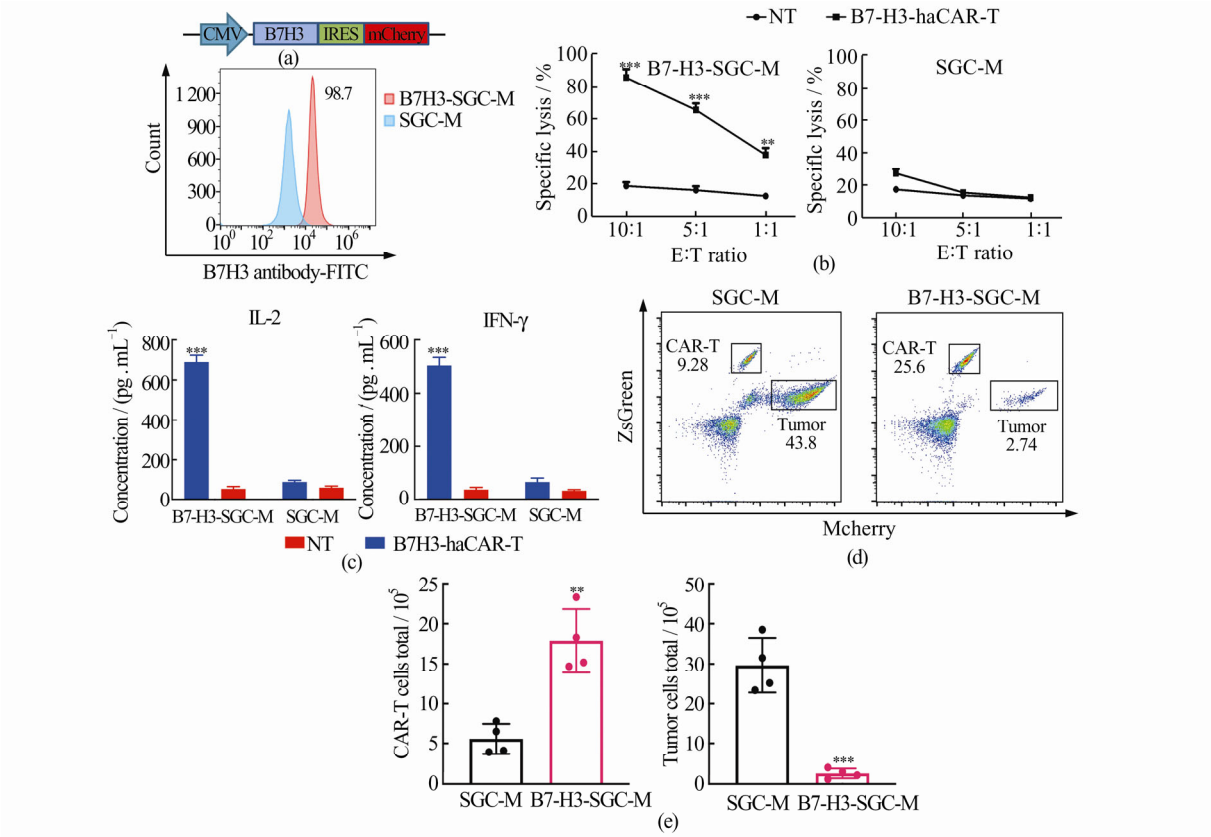

Fig. 2 Anti-tumor efficacy of B7-H3-haCAR-T cells *in vitro*

(a) Schematic representation of DNA structures for the construction of B7-H3-Mcherry fusion proteins; flow cytometric assay of B7-H3 from SGC-Mcherry cells and B7-H3-SGC-Mcherry cells with a FITC labeled anti-B7-H3 monoclonal antibody; (b) ^{51}Cr-release assays of haCAR-T cells against B7-H3-SGC-Mcherry or SGC-Mcherry cell at different E:T proportions; (c) The IFN-γ and IL-2 secretion levels of haCAR-T cells co-incubated with target cells in E:T proporation of 5:1 at 8 h were measured through ELISA; (d) Representative flow cytometer dot plots displaying haCAR-T cells and tumor cells after 72 h of co-incubated; (e) Absolute numbers of haCAR-T cells and tumor cells after 72 h of co-incubated ($^{**}P$<0.01, $^{***}P$<0.001)

B7-H3-haCAR-T cells through the caudal vein and tumor growth was monitored every two days (The treat ment schema is shown in Fig. 3(a)). As expected, mice treated with B7-H3-haCAR-T cells demonstrated a noteworthy inhibition in tumor enlargement in contrast with untransduced control T cells and PBS groups (Fig. 3(b)). In addition, as shown in the total antioxidant status (TAs) graph (Fig. 3(c)), the survival in the xenograft mouse model treated with B7-H3-haCAR-T cells was much longer than other groups. Together these results showed that compared with PBS and control T cells, B7-H3-haCAR-T cells can effectively infiltrate the tumor tissues and have a significant killing effect on tumor cells.

Off-target toxicity is one of the serious side-effects of CAR-T therapy. In order to verify the safety of B7-H3-haCAR-T cells, we performed hematoxylin- eosin (HE) staining of the major tissues of mice executed 10 days after injection of PBS, T and B7-H3-haCAR-T, respectively, to further observe the effect of B7-H3-haCAR-T cells on normal tissues. As shown in Fig. 3(d), major tissues had no obvious histo-pathological abnormalities or lesions in the B7-H3-haCAR-T treated group, which suggested that there was no evidence of off-target toxicity caused by B7-H3-haCAR-T cells.

3 Discussion

CAR-T is a promising cancer treatment in recent years and two products targeting CD19 for refractory/relapsed B-cell malignancies have been approved by the Food and Drug Administration (FDA) in 2017 and 2018[25, 26]. However, the vast structural differences between solid tumors and hematological tumors make majority of the patients with solid tumors ineffective to CAR-T therapies[27]. The tumor microenvironment, which is unique to solid tumors, leads to rapid apoptosis of CAR-T cells, which is one of the key factors limiting CAR-T treatment for solid tumors[28]. Recent evidence suggests that further optimization of CAR structure can

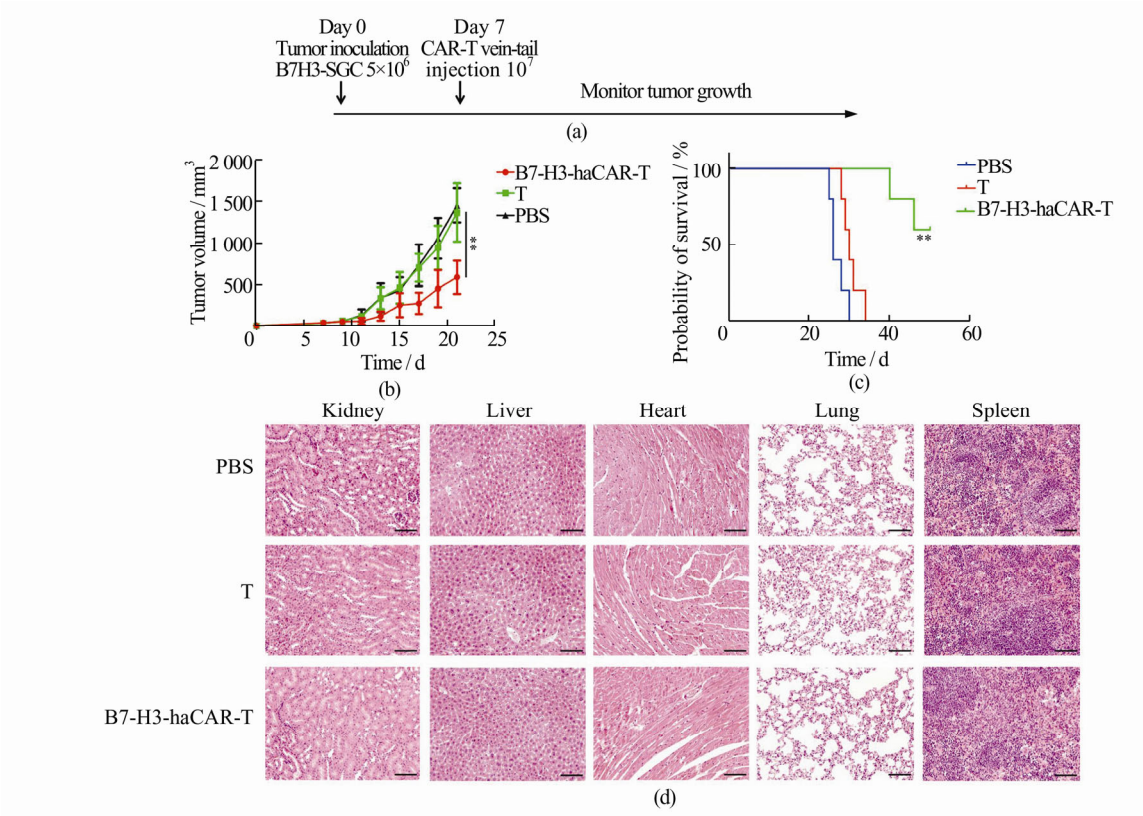

Fig. 3 Antitumor efficacy and safety evaluation of B7-H3-haCAR-T cells *in vivo*

(a) Schematic diagram of the xenograft model treatment protocol; (b) Volumetric measurement of xenograft tumors in each group at the indicated time; (c) Measurement of survival curves in mice by the Kaplan-Meier method; (d) The main organs of the treated mice were stained with hematoxylin and eosin (H&E); $^{**}P < 0.01$

improve the tumour-killing effect of CAR-T, prolong its survival time *in vivo* and can effectively resist the side effects of the tumour microenvironment on CAR-T[29]. Humanized scFv have been noted to give better recognition specificity and anti-tumor capacity to CAR-T cells compared to murine scFv which could bring more meaningful improvements in the treatment of solid malignancies with CAR-T[30].

The precise therapeutic target plays pivotal role to the security and efficacy of CAR-T treatment[31]. CD19 CAR-T cells have shown significant efficacy in the therapy of leukemia, but no cell surface antigen with similar properties to CD19 has been found in solid tumors[32]. The off-target toxicity is observed when selecting molecules such as HER2 or EGFR for CAR-T treatment of solid tumors, as these molecules are also expressed in some normal tissues[33, 34]. The ideal CAR targeting molecule should be mainly overexpressed on the surface of cancer cells, with very low or zero expression in normal tissues[35]. To date, B7-H3 molecule has been proved to be specifically and broadly overexpressed on tumor tissues which have negative immune regulation function, and thus tumor cells can escape the human immune surveillance by applying this mechanism[36]. Further comprehension of the role of B7-H3 and added preclinical and clinical exploration may identify it as a reasonable anti-tumor target.

In this study, we prepared a B7-H3-haCAR with humanized scFv derived from hu8H9mAb to target B7-H3 which is specifically enriched on the surface of tumor cells. The 8H9mAb was humanized by grafting the heavy and light chain CDR loops of 8H9scFv onto the human IgG1 framework. The new humanized 8H9 (hu8H9) scFv was further mutation-optimized by adopting yeast display technology to achieve a 160-fold increased affinity to B7-H3 compared to the previously reported one[24]. Our cytotoxic experiments revealed that the increased affinity of humanized scFv has benefited the B7-H3-haCAR-T cells to maintain its tumor killing effect even at a lower E:T ratio (Fig. 2(d)). This clearly showed that even low doses of B7-H3-haCAR-T could be used for clinical treatment which in turn would effectively avoid the occurrence of cytokine-released syndrome (CRS).

However, it should be taken into account that this study has only checked the antitumor efficacy of the B7-H3-haCAR-T with B7-H3 over expressed modified SGC (B7-H3-SGC-Mcherry). Further detailed study on the effect of B7-H3-haCAR-T cells over other B7-H3 overexpressed wild type (WT) cancer cells and added evaluation studies of its effectiveness and safety on patient-derived tumor xenografts (PDXs) model could make this B7-H3-haCAR-T cells more opt for treatment of solid tumors in future.

4 Conclusion

We developed humanized B7-H3-haCAR-T cells which have prominent cytotoxic effects on B7-H3-SGC-Mcherry cells *in vitro* and obviously exerted tumour remission in xenograft tumor models and hence our results support the clinical development of humanized B7-H3-haCAR-T in solid tumors.

References

[1] Cheadle E J, Sheard V, Hombach A A, *et al*. Chimeric antigen receptors for T-cell based therapy[J]. *Methods in Molecular Biology* (*Clifton*, *N J*), 2012, **907**: 645-666.

[2] McDonald D, Stockwin L, Matzow T, *et al*. Coxsackie and adenovirus receptor (CAR)-dependent and major histocompatibility complex (MHC) class I-independent uptake of recombinant adenoviruses into human tumour cells [J]. *Gene Therapy*, 1999, **6**(9): 1512-1519.

[3] Fujiwara K, Masutani M, Tachibana M, *et al*. Impact of scFv structure in chimeric antigen receptor on receptor expression efficiency and antigen recognition properties [J]. *Biochemical and Biophysical Research Communications*, 2020, **527**(2): 350-357.

[4] Feins S, Kong W M, Williams E F, *et al*. An introduction to chimeric antigen receptor (CAR) T-cell immunotherapy for human cancer[J]. *American Journal of Hematology*, 2019, **94**(S1): S3-S9.

[5] Chavez J C, Yassine F, Sandoval-Sus J, *et al*. Anti-CD19 chimeric antigen receptor T-cell therapy in B-cell lymphomas: Current status and future directions [J]. *International Journal of Hematologic Oncology*, 2021, **10**(2): IJH33.

[6] Kershaw M H, Westwood J A, Parker L L, *et al*. A phase I study on adoptive immunotherapy using gene-modified T cells for ovarian cancer [J]. *Clinical Cancer Research*: *An Official Journal of the American Association for Cancer Research*, 2006, **12**(20 Pt 1): 6106-6115.

[7] Song D G, Ye Q R, Poussin M, *et al*. A fully human chimeric antigen receptor with potent activity against cancer cells but reduced risk for off-tumor toxicity [J]. *Oncotarget*, 2015, **6**(25): 21533-21546.

[8] Zhao Y, Liu Z F, Wang X, *et al*. Treatment with humanized selective CD19CAR-T cells shows efficacy in highly treated B-ALL patients who have relapsed after receiving murine-based CD19CAR-T therapies [J]. *Clinical Cancer Research*: *An Official Journal of the American Association for Cancer Research*, 2019, **25**(18): 5595-5607.

[9] Chapoval A I, Ni J, Lau J S, *et al*. B7-H3: A costimulatory molecule for T cell activation and IFN-γ production [J]. *Nature Immunology*, 2001, **2** (3): 269-274.

[10] Seaman S, Zhu Z Y, Saha S, *et al*. Eradication of tumors through simultaneous ablation of CD276/B7-H3-positive tumor cells and tumor vasculature[J]. *Cancer Cell*, 2017, **31**(4): 501-515.

[11] Inamura K, Yokouchi Y, Kobayashi M, *et al*. Tumor B7-H3 (CD276) expression and smoking history in relation to lung adenocarcinoma prognosis [J]. *Lung Cancer*, 2017, **103**: 44-51.

[12] Benzon B, Zhao S G, Haffner M C, *et al*. Correlation of B7-H3 with androgen receptor, immune pathways and poor outcome in prostate cancer: An expression-based analysis [J]. *Prostate Cancer and Prostatic Diseases*, 2017, **20**(1): 28-35.

[13] Parker A S, Heckman M G, Sheinin Y R, *et al*. Evaluation of B7-H3 expression as a biomarker of biochemical recurrence after salvage radiation therapy for recurrent prostate cancer[J]. *International Journal of Radiation Oncology Biology Physics*, 2011, **79**(5): 1343-1349.

[14] Loos M, Hedderich D M, Ottenhausen M, *et al*. Expression of the costimulatory molecule B7-H3 is associated with prolonged survival in human pancreatic cancer [J]. *BMC Cancer*, 2009, **9**: 463.

[15] Souweidane M M, Kramer K, Pandit-Taskar N, *et al*. Convection-enhanced delivery for diffuse intrinsic pontine glioma: A single-centre, dose-escalation, phase 1 trial [J]. *The Lancet Oncology*, 2018, **19**(8): 1040-1050.

[16] Ni L, Dong C. New checkpoints in cancer immunotherapy [J]. *Immunological Reviews*, 2017, **276**(1): 52-65.

[17] Modak S, Kramer K, Gultekin S H, *et al*. Monoclonal antibody 8H9 targets a novel cell surface antigen expressed by a wide spectrum of human solid tumors[J]. *Cancer Research*, 2001, **61**(10): 4048-4054.

[18] Luther N, Cheung N K V, Dunkel I J, *et al*. Intraparenchymal and intratumoral interstitial infusion of anti-glioma monoclonal antibody 8H9 [J]. *Neurosurgery*, 2008, **63**(6): 1166-1174.

[19] Modak S, Guo H F, Humm J L, *et al*. Radioimmunotargeting of human rhabdomyosarcoma using monoclonal antibody 8H9 [J]. *Cancer Biotherapy & Radiopharmaceuticals*, 2005, **20**(5): 534-546.

[20] Kramer K, Kushner B H, Modak S, *et al*. Compartmental intrathecal radioimmunotherapy: Results for treatment for metastatic CNS neuroblastoma [J]. *Journal of Neuro-Oncology*, 2010, **97**(3): 409-418.

[21] Zhou Z P, Luther N, Ibrahim G M, *et al*. B7-H3, a potential therapeutic target, is expressed in diffuse intrinsic pontine glioma [J]. *Journal of Neuro-Oncology*, 2013, **111**(3): 257-264.

[22] Bartholomä M D. Radioimmunotherapy of solid tumors: Approaches on the verge of clinical application [J]. *Journal of Labelled Compounds and Radiopharmaceuticals*, 2018, **61**(9): 715-726.

[23] Tang X, Zhao S S, Zhang Y, *et al*. B7-H3 as a novel CAR-T therapeutic target for glioblastoma [J]. *Molecular Therapy - Oncolytics*, 2019, **14**: 279-287.

[24] Ahmed M, Cheng M, Zhao Q, *et al*. Humanized affinity-matured monoclonal antibody 8H9 has potent antitumor activity and binds to FG loop of tumor antigen B7-H3 [J]. *Journal of Biological Chemistry*, 2015, **290**(50): 30018-30029.

[25] Maude S L, Frey N, Shaw P A, *et al*. Chimeric antigen receptor T cells for sustained remissions in leukemia [J]. *The New England Journal of Medicine*, 2014, **371**(16): 1507-1517.

[26] Kochenderfer J N, Dudley M E, Kassim S H, *et al*. Chemotherapy-refractory diffuse large B-cell lymphoma and indolent B-cell malignancies can be effectively treated with autologous T cells expressing an anti-CD19 chimeric antigen receptor [J]. *Journal of Clinical Oncology*: *Official Journal of the American Society of Clinical Oncology*, 2015, **33**(6): 540-549.

[27] Hou B, Tang Y, Li W H, *et al*. Efficiency of CAR-T therapy for treatment of solid tumor in clinical trials: A meta-analysis [J]. *Disease Markers*, 2019, **2019**: 3425291.

[28] Martinez M, Moon E K. CAR T cells for solid tumors: New strategies for finding, infiltrating, and surviving in the tumor microenvironment [J]. *Frontiers in Immunology*, 2019, **10**: 128.

[29] Li J, Li W W, Huang K J, *et al*. Chimeric antigen receptor T cell (CAR-T) immunotherapy for solid tumors: Lessons learned and strategies for moving forward [J]. *Journal of Hematology & Oncology*, 2018, **11**(1): 22.

[30] Wang K, Zhao Y, Wang X, *et al*. Case report: Humanized selective CD19CAR-T treatment induces MRD-negative remission in a pediatric B-ALL patient with primary resistance to murine-based CD19CAR-T therapy [J]. *Frontiers in Immunology*, 2020, **11**: 581116.

[31] Yu S N, Li A P, Liu Q, *et al*. Chimeric antigen receptor T cells: A novel therapy for solid tumors [J]. *Journal of Hematology & Oncology*, 2017, **10**(1): 78.

[32] Titov A, Valiullina A, Zmievskaya E, *et al.* Advancing CAR T-cell therapy for solid tumors: Lessons learned from lymphoma treatment [J]. *Cancers*, 2020, **12**(1): 125.

[33] Lamers C H, Sleijfer S, van Steenbergen S, *et al*. Treatment of metastatic renal cell carcinoma with CAIX CAR-engineered T cells: Clinical evaluation and management of on-target toxicity [J]. *Molecular Therapy*, 2013, **21**(4): 904-912.

[34] Caruso H G, Hurton L V, Najjar A, *et al*. Tuning sensitivity of CAR to EGFR density limits recognition of normal tissue while maintaining potent antitumor activity [J]. *Cancer Research*, 2015, **75**(17): 3505-3518.

[35] Newick K, O'Brien S, Moon E, *et al*. CAR T cell therapy for solid tumors [J]. *Annual Review of Medicine*, 2017, **68**(11): 139-152.

[36] Yang S, Wei W, Zhao Q. B7-H3, a checkpoint molecule, as a target for cancer immunotherapy [J]. *International Journal of Biological Sciences*, 2020, **16**(11): 1767-1773.

□